Draft version September 2, 2025
Typeset using LaTeX **twocolumn** style in AASTeX631

Planetesimal formation by gravitational collapse on the back of an envelope

S. Paine,[1] N. Magnan,[2] and A. N. Youdin[3,4]

[1] *Astronomy Unit, School of Physics and Astronomy, Queen Mary University of London, London E1 4NS, United Kingdom*
[2] *Laboratoire Lagrange, Observatoire de la Côte d'Azur, Université de la Côte d'Azur, Nice, France*
[3] *Department of Astronomy and Steward Observatory, University of Arizona, Tucson, Arizona 85721, USA*
[4] *The Lunar and Planetary Laboratory, University of Arizona, Tucson, Arizona 85721, USA*

ABSTRACT

The metre-size barrier remains an open problem in the field of planetesimal formation. Various mechanisms have been proposed to allow cm-sized grains to overcome barriers to their growth into kilometre-sized objects. A common theme amongst many of these mechanisms is the local concentration of dust to very high dust-to-gas ratios. We approach the problem of gravitation collapse in high dust-to-gas regimes in a methodic, first-order fashion to build a general picture of the physics involved at each step of the collapse. At the beginning of the collapse, we find that incoming gas from the disc is not able to strip significant amounts of material from the starting dust clump, so collapse can occur in dust clumps up to a Hill radius in size. We also find that the dust and gas should remain isothermal to first-order during the entire collapse process, as well as remaining at equal temperatures to one another. Finally, we find that incoming gas turbulence from the disc should not be present inside the dust clump during collapse, but cannot yet comment on other sources of turbulence.

Keywords: dust, planetesimal formation, turbulence

1. INTRODUCTION

According to the MPC, there are 1,457,773 minor bodies discovered as of the writing of this paper, and many millions other asteroids, comets and other leftover material from the Solar System's planet formation era. Their formation mechanism remains a mostly open question, however. This is an important process to physically constrain, as it ties together processes early in a disc's lifetime to the planets and minor bodies that dominate the disc later on.

The need for a mechanism for planetesimal formation stems from the so called 'metre-sized barrier' - where grains can grow up to cm-size before their collisions tend to cause fragmentation, rather than growth (Birnstiel et al. 2011). On the other end of this, once objects reach km-size, they can grow via gravitational accretion (Lissauer & Stewart 1993) or pebble accretion (Ormel & Klahr 2010). This still leaves 5 orders of magnitude in size that needs to be overcome. Dust clump forming mechanisms, such as the streaming instability are possible solutions to this problem (Youdin & Goodman (2005) and Youdin & Johansen (2007)), as they concentrate dust in high dust-to-gas environments, allowing them to potentially overcome these fragmentation barriers. A better study of how initial clump conditions affect the final planetesimals formed could help distinguish valid clump forming mechanisms. Another potentially observable effect of the collapse mechanism is in the properties of asteroids observed today. From their binary fraction (e.g. Morbidelli & Nesvorny (2020)), porosity and composition (e.g. Cuzzi et al. (2010) and Kobayashi & Tanaka (2021)).

In this paper, we will approach this matter with order of magnitude estimates and first-order contributions from the various physical processes we expect to be relevant. This is to gain an intuitive sense of which physics are important at the various stages of collapse of a dust clump and how this creates planetesimals. The goal is that by providing a framework for the entire collapse process, and the important physics at each stage, future analytical and computational models can be improved. We will also attempt to gain some insight into how this can inform current and future observations, in hopes of distinguishing between clump formation mechanisms. We will start by establishing the minimum starting size for a dust clump before collapse, we then look at the timescale of the overall collapse, the thermodynamics and aerodynamics involved and finally discuss turbulent processes inside the dust clump.

2. COLLAPSE CRITERION

2.1. *Hill radius*

The Hill radius of a given body describes the distance to which its gravitational influence dominates in an N-body system. Outside of this radius, regardless of any gas in the disc, a clump of dust would not be able to gravitationally hold on to material outside of this radius. Instead, it would be tidally stripped by the central star. In the case of two bodies, it can trivially be derived by balancing gravitational forces, giving:

$$R_H = r\left(\frac{M}{3M_*}\right)^{1/3}. \tag{1}$$

For material within the Hill radius to be able to escape, it must have an 'escape' velocity large enough to overcome the gravitational potential keeping it within the Hill sphere. This 'Hill escape' velocity can be derived by looking at the gravational energy:

$$\frac{1}{2}v^2_{\rm Hill,esc}(r) = -\frac{GM}{R_H} - \frac{-GM}{r} \tag{2}$$

$$v_{\rm Hill,esc}(r) = \sqrt{2GM\left(\frac{1}{r} - \frac{1}{R_H}\right)}. \tag{3}$$

In the case of material starting at the clump radius, we get the minimum velocity needed for it to become gravitationally unbound from the clump:

$$v_{\rm Hill,esc} = \sqrt{2GM\left(\frac{1}{R_c} - \frac{1}{R_H}\right)}. \tag{4}$$

2.2. *Erosion*

While in the disc, the dust clump will experience a number of gas wind forces, which can strip it of material. This will reduce the starting radial size and mass of the clump. Below we will discuss three such sources of wind, but first we will describe the mechanism by which this can remove material from the clump. Finally, we will use this to set a bound on how much smaller than the Hill radius a dust clump needs to be to avoid any significant erosion mass loss.

Gas entering the dust clump will start colliding inelastically with the dust grains present there, and as they do they must conserve the momentum of the system (but not mechanical energy). From this, we can derive the outgoing velocity of the gas and dust combined, which we call $v_{\rm eros}$:

$$(\rho_g + \rho_d)\, v_{\rm eros} = \rho_g v_{\rm wind} \tag{5}$$

$$v_{\rm eros} = \frac{\rho_g}{\rho_0} v_{\rm wind}. \tag{6}$$

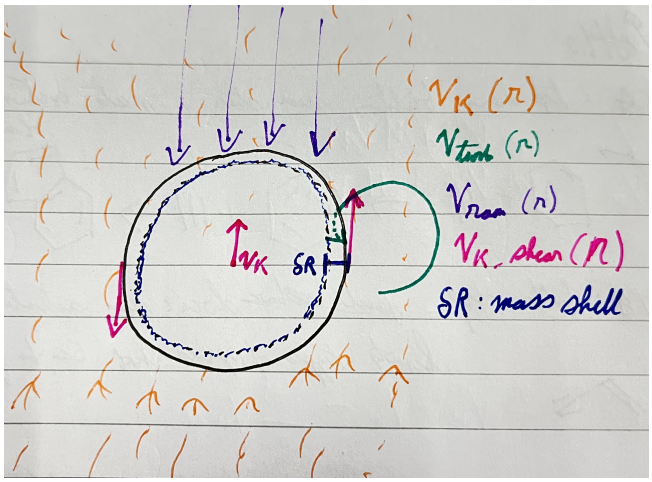

Figure 1. Diagram of three different gas wind forces that can strip a dust clump of its material.

For the incoming gas to strip material out to the Hill radius, the final erosion velocity must be greater than the Hill escape velocity ($v_{\rm eros} \geq v_{\rm Hill,esc}$). Since we are in an environment where the dust-to-gas ratio is large ($\delta_{\rm d2g} \gg 1$), the incoming gas needs velocities much higher than this escape velocity to have enough momentum to strip material.

2.2.1. *Turbulent contribution*

Shariff & Cuzzi (2015) point out that turbulent eddies exert a strain on the clump, possibly eroding it. Eddy velocity is positively correlated to eddy size, but eddies larger than the clump exert a ram pressure rather than a strain. Therefore, the largest strain rate should originate from the clump-scale eddies. We shall see in §7.1 that the turbulent velocity at this scale is of order

$$\begin{aligned} v_{\rm turb} &= v_f \left(\frac{R_c}{l_f}\right)^{1/3} \\ &= \alpha^{1/3}\left(\frac{R_0}{H}\right)^{1/3} c_{\rm s} \end{aligned}$$

$$v_{\rm turb,clump} = 5.5\left(\frac{\alpha}{10^{-4}}\right)^{1/3} X_0^{-\frac{(2q+1)}{6}} \left(\frac{r}{1\,\rm AU}\right)^{-\frac{(2q+1)}{6}} \text{m/s}, \tag{7}$$

$$v_{\rm turb} = 8.0\left(\frac{r}{1\,\rm AU}\right)^{-\frac{(2q+1)}{6}} \text{m/s} \tag{8}$$

where $c_{\rm s}$ is the sound speed. At $r = 1\,\rm AU$, this only amounts to about 5.5 m/s, making it unable to overcome the Hill escape velocity at any meaningful time during the collapse. So, overall, we conclude that this

2.2.2. *Contribution of the headwind*

In this section we consider the radial and azimuthal effects of gas drag on the dust clump from the sub-Keplerian gas. The gas orbits at sub-Keplerian velocities because it is supported by a pressure gradient, while the dust orbits at the Keplerian velocity, creating a velocity difference. With its high dust to gas ratio, we expect the dust clump to aerodynamically behave as a single large object, rather than many individual small grains. This firmly puts us in the turbulent drag regime. The equations for this are:

$$v_{g,r} = 0 \tag{9a}$$
$$v_{g,\phi} = (1-\eta)\, v_k \tag{9b}$$
$$v_{d,r} = -\frac{2\eta\,\mathrm{St}}{1+\mathrm{St}^2} v_k \tag{9c}$$
$$v_{d,\phi} = \left(1 - \frac{\eta}{1+\mathrm{St}^2}\right) v_k \tag{9d}$$

Where $\eta \sim \left(\frac{c_s}{v_k}\right)^2$ is the pressure gradient and the Stokes' number $\mathrm{St} \equiv \Omega\tau_s$ Subtracting the dust velocities from the gas velocities, we get the difference between the two:

$$\Delta v_r = \frac{2\eta v_k\,\mathrm{St}}{1+\mathrm{St}^2} \tag{10a}$$
$$\Delta v_\phi = -\frac{\eta\,\mathrm{St}^2 v_k}{1+\mathrm{St}^2} \tag{10b}$$

We find these two line up when $\mathrm{St} = 2$. Taking their ratios also illuminates which direction the ram pressure dominates for which sized grains:

$$\left|\frac{\Delta v_\phi}{\Delta v_r}\right| = \frac{\mathrm{St}}{2} \tag{11}$$

From this we can see that the azimuthal ram pressure dominates for large Stokes' numbers, while the radial ram pressure term dominates for small Stokes' numbers. In our case, since we have very large Stokes' numbers ($\mathrm{St} \gg 1$, we expect the radial drag contribution to be negligible and can simplify the azimuthal velocity difference:

$$\Delta v_\phi \simeq -\eta v_k. \tag{12}$$

Putting some numbers to this, we find

$$\Delta v_\phi \sim -r^{-q+1}$$
$$\Delta v_\phi = -21.4 \left(\frac{r}{1\,\mathrm{AU}}\right)^{-q+1/2} \mathrm{m/s}. \tag{13}$$

Of the three main sources of gas drag, this is the most important contribution.

2.2.3. *Contribution of the Keplerian shear*

As mentioned in previous sub-subsection, we expect the clump to behave like a single large solid. As a result, the whole will move at the Keplerian orbital velocity of its centre of mass. For a large enough clump, the edges of the clump will experience a different Keplerian orbital velocity than the centre of the clump - imparting a drag force on the material on those edges. This is what we are calling a 'Keplerian shear', as the velocity difference is in opposite directions between the inner and outer parts of the clump, relative to the central star. Using the Keplerian velocity gives an upper bound on these velocity differences and therefore the drag

$$\Delta v_{k,\mathrm{outer}} = v_k(r) - v_k(r+R_c) = \sqrt{\frac{GM}{r}} - \sqrt{\frac{GM}{r+R_c}} \tag{14a}$$
$$\Delta v_{k,\mathrm{inner}} = v_k(r) - v_k(r-R_c) = \sqrt{\frac{GM}{r}} - \sqrt{\frac{GM}{r-R_c}}. \tag{14b}$$

The outer Keplerian velocity shear will always be the bigger of the two, so using this as an upper limit, we can derive the velocity contribution from this:

$$\Delta v_k = 1.3 \left(\frac{r}{1\,\mathrm{AU}}\right)^{-1/2} \mathrm{m/s}. \tag{15}$$

2.2.4. *Conclusion*

As previously stated, the most important contribution to gas drag is the azimuthal drift velocity. However, we can set an upper bound on all the forces combined to set a minimum clump size for which we can ignore any mass loss due to erosion. Assuming all the velocities combine constructively, we get a total gas velocity:

$$v_{\mathrm{tot}} = \sqrt{v^2_{\mathrm{turb,clump}} + \Delta v_r^2 + \Delta v_\phi^2 + \Delta v^2_{k,\mathrm{outer}}} \tag{16}$$
$$\sim \Delta v_\phi\,. \tag{17}$$

This can only entrain material if $v_{\mathrm{tot}} \geq v_{\mathrm{Hill,esc}}$. Putting in numbers, we will consider this velocity at three different points in the disc

r (AU)	$X_0 R_H$ where $v_{\mathrm{tot}} < v_{\mathrm{Hill,esc}}$
1.0	0.99
10.0	0.95
100.0	0.72

The exact Hill radius fraction for which material can no longer be entrained can be exactly solved by finding where the total velocity equals the Hill escape velocity. As the clump collapses, the Hill escape velocity

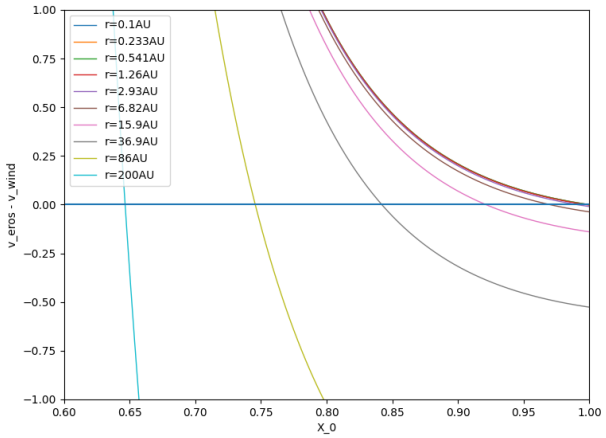

Figure 2. Fraction of the Hill radius where the various wind velocities are no longer able to erode material from the clump. $v_{\rm wind} < v_{\rm eros}$ when the lines cross zero. The values of X_0 are given for a selection of starting orbital radii.

increases, but the gas forces remain largely constant.

$$v_{tot} \sim \Delta v_\phi = \frac{\rho_0}{\rho_g} v_{\rm Hill,\ esc} \quad (18)$$

$$\Delta v_\phi \sim -\eta v_k \quad (19)$$

$$\rho_0 \simeq \rho_d \quad (20)$$

$$\frac{8\pi^2[c_s(r)]^2[\Sigma_g(r)]^2[R_H(r)]^7}{9Gr^2[M(R_p)]^3} = \frac{1-X_0}{X_0^7} \quad (21)$$

This 7th order polynomial must be solved numerically, and a figure containing some starting orbital radii 2 is provided. An important thing to note is that for starting radii below 10 AU, the Hill fraction is more than 90%. Plugging in some numbers, we find a scaling relation for this Hill fraction solution:

$$0.013 \left(\frac{r}{1\,\mathrm{AU}}\right)^{5-2p-q} \left(\frac{R_p}{10^5\,\mathrm{m}}\right)^{-2} = \frac{1-X_0}{X_0^7} \quad (22)$$

From this we can see that in the inner disc, any material within the Hill radius is strongly gravitationally bound, and the various gas forces in the surrounding disc shouldn't be strong enough to drive any significant mass loss once the clump has begun collapsing. However, in the outer disc, this is more complicated, and depending on how long the collapse takes, a significant amount of the mass might be stripped from the clump into the surrounding disc. The following sections will discuss these timescales in more detail.

2.3. *Caveats*

There are some limitations and assumptions with the derivations we have made above. One important one is that we assume the dust has zero initial velocity. If the collapse has started and the dust has an inwards velocity - removing mass will be even more difficult than stated above. However, if it has any random motion that is outwards, this will make it easier for material to be liberated. However, this latter case probably isn't relevant if we are in the drag-limited regime, as this would damp any dust motion.

3. TIMESCALES

3.1. *Free-fall timescale*

Consider a spherical shell of radius R enclosing a mixture of gas and pebbles of total mass M. If the shell is only subject to gravity, its evolution is governed by

$$\frac{\mathrm{d}^2 R}{\mathrm{d}t^2} = -\frac{GM}{R^2}.$$

If the shell is initially at rest, conservation of energy quickly gives

$$\frac{\mathrm{d}R}{\mathrm{d}t} = -\sqrt{2\,GM\left(\frac{1}{R} - \frac{1}{R_0}\right)} \quad (23)$$

(Using the integration trick: $\frac{d}{dt} = \frac{d}{dR}\frac{dR}{dt} = v\frac{d}{dR}$). Integrating this velocity from R_0 to 0 give us the free-fall time $t_{\rm ff}$:

$$\int_0^{R_0} \frac{ds}{\sqrt{2\,GM\left(\frac{1}{s} - \frac{1}{R_0}\right)}} = \int_0^{t_{\rm ff}} dt,$$

In fine, we get

$$t_{\rm ff} = \frac{\pi}{2}\sqrt{\frac{R_0^3}{2\,GM}} = 3.2 \times 10^6\, X_0^{3/2} \left(\frac{r}{1\,\mathrm{AU}}\right)^{3/2} \mathrm{s}. \quad (24)$$

Note that the parameters we use when computing numeric values are listed in §A.

3.2. *Collapse timescale*

In Segretain et al. (2024), they derive a collapse time assuming an initial static gas that collapses at terminal velocity and find this matches simulations quite accurately. We quote their collapse time here:

$$t_{\rm c} = \frac{R_0^3}{3GMt_s} \quad (25)$$

$$= 4.5 \times 10^8 \left(\frac{a}{1\,\mathrm{cm}}\right)^2 X_0^3 \left(\frac{r}{1\,\mathrm{AU}}\right)^{3/2-p} \mathrm{s}. \quad (26)$$

This gives a slower collapse time than the free-fall time by about 2 orders of magnitude in the inner disc.

3.3. *Sound crossing time*

We show in §B that in a well-coupled dust/gas mixture like our clump, the sound speed is slower than usual. One way to understand this is to think that the mean molecular weight is increased by the dust particles. Accounting for this effect, we find that the sound crossing time of the clump is

$$t_\mathrm{s} = \sqrt{\mu+1}\,\frac{R_0}{c_\mathrm{s}} = 1.5\times10^5\,\left(\frac{r}{1\mathrm{AU}}\right)^{p+q/2-2}\left(\frac{R_\mathrm{p}}{10^5\mathrm{m}}\right)\mathrm{s}, \tag{27}$$

where R_p is the radius of the final planetesimal.

3.4. *Caveats*

Our collapse timescale estimate relies on the assumption of static gas and terminal velocity. We shall determine whether those assumptions are valid in §6.

4. TEMPERATURES

4.1. *Do the grains have a well-defined temperature?*

The thermal diffusivity of silicates is of order $\kappa_\mathrm{s} = 1.4\times10^{-6}\,\mathrm{m}^2/\mathrm{s}$, so the largest grains will take

$$t_\mathrm{dif.} = \frac{a^2}{\kappa_\mathrm{s}} = 71\,\left(\frac{a}{1\,\mathrm{cm}}\right)^2\,\mathrm{s} \tag{28}$$

to homogenize their temperature.

This is much shorter than the free-fall timescale, so any heat that goes into the grains will spread over their volume rather than just their surface. Most solids have a similar thermal diffusivity to silicate, so this prediction should not be affected by composition.

4.2. *Do grains and gas have the same temperature?*

Grains are constantly colliding with dihydrogen molecules, and each collision induces a small exchange of energy. When the gas number density is high, collisions are frequent, so the exchange of energy is fast enough that dust and gas rapidly equilibrate to the same temperature. But if the gas density is low enough, dust and gas temperatures can differ.

Haberle et al. (2025) propose the following estimates for the time it takes collisional exchanges to affect the gas and dust temperatures

$$t_{\mathrm{ex;\,g}} \approx \frac{c_{\mathrm{p,g}}\,\rho_\mathrm{g}}{3\pi\,a^2 c_\mathrm{s} k_\mathrm{B} n_\mathrm{g} n_\mathrm{d}},$$
$$t_{\mathrm{ex;\,d}} \approx \frac{c_{\mathrm{p,s}}\,\rho_\mathrm{d}}{3\pi\,a^2 c_\mathrm{s} k_\mathrm{B} n_\mathrm{g} n_\mathrm{d}},$$

where n denotes a number density, ρ a standard density, c_p a specific heat capacity, and k_B Boltzmann's constant.

The heat capacity of dihydrogen is higher than that of silicates, but the dust-to-gas ratios within collapsing clumps are high. To get an upper bound on the exchange timescales, we consider the gas and dust densities at the start of the collapse. We get

$$t_{\mathrm{ex;\,g}} = 44\,\left(\frac{a}{1\,\mathrm{cm}}\right) X_0^3 \left(\frac{r}{1\,\mathrm{AU}}\right)^{q/2+3}\,\mathrm{s}, \tag{29a}$$
$$t_{\mathrm{ex;\,d}} = 3.0\times10^2\,\left(\frac{a}{1\,\mathrm{cm}}\right)\left(\frac{r}{1\,\mathrm{AU}}\right)^{p+3/2}\,\mathrm{s}, \tag{29b}$$

where $X = R/R_\mathrm{H}$ is a fudge factor describing the current size of the clump relative to the Hill radius.

Those timescales are much shorter than the free-fall timescale, so we expect the dust and the gas to always have the same temperature.

4.3. *Is the system isothermal?*

As the clump collapses, it releases gravitational potential energy. If the the clump is initially spherical and of uniform density, we have

$$\mathcal{G} = \frac{3}{5}\frac{GM^2}{R_0},$$

Ultimately, most of this energy will be converted to heat.

But to get an upper bound on the temperature difference, let us assume that all the gravitational potential energy of the clump is converted into heat. Most of the mass is in the grains, and we saw in the previous subsections that even if the dissipative processes were to only heat up the gas, this heat will quickly sink into the grains. The specific heat capacity of silicates is lower than that of water ice, so the maximum warm-up we can hope to observe is

$$\Delta T = \frac{\mathcal{G}}{M\,c_{\mathrm{p,s}}} = 10^{-2} X_0^{-1}\,\left(\frac{r}{1\,\mathrm{AU}}\right)^{-1}\left(\frac{R_\mathrm{p}}{10^5\,\mathrm{m}}\right)^2\,\mathrm{K}. \tag{30}$$

This is tiny compared to melting or sublimation temperatures, so the collapse is unlikely to allow for late differentiation, nor to leave an observable imprint onto the chemical and mineralogical composition of comets, asteroids and meteorites.

4.4. *Caveats*

In our derivation, we ignore any possible effects of dust grain porosity. Another important thing to consider is that while the overall temperature should remain quite unaffected, high levels of local heating, for example on the planetesimal surface due to collisions, could lead to non-isothermal conditions.

5. DRAG

5.1. *Are we in the linear drag regime?*

To answer this question, we need to evaluate the Mach number of the particles. If it is much lower than unity, we can use the linear drag laws (Hopkins & Squire 2018).

Several typical velocities could be considered, so get an upper bound on the Mach number, we can assume that the entire gravitational potential energy contained by the clump is transformed into kinetic energy. If all the particles have the same mass, the average particle velocity is

$$v = \sqrt{\frac{2\mathcal{G}M}{R_0}}.$$

By plugging in some numbers for M and R_0, we get

$$v = 6.5 \left(\frac{r}{1\,\mathrm{AU}}\right)^{-1/2} \left(\frac{R_\mathrm{p}}{10^5\,\mathrm{m}}\right) \mathrm{m/s}. \tag{31}$$

Wherever we are in the disc, this velocity remains much lower than the sound speed, so we can safely use the linear drag laws.

5.2. *Stokes or Epstein?*

If the particles are smaller than the gas' mean free path, we are in the Epstein drag regime. Otherwise, we need to use the Stokes' or turbulent drag laws (Weidenschilling 1977).

5.2.1. *Start of the collapse*

At the start of the collapse, the gas density is set by the disc model. We find that[1]

$$\frac{9}{4}\lambda = 3.6\times10^{-3} \left(\frac{r}{1\,\mathrm{AU}}\right)^{p+3/2-q/2} \mathrm{m}. \tag{32}$$

There is much uncertainty regarding the size of the largest grains at the end of the clump formation processes, but for silicate grains one can argue that fragmentation makes grains larger than 1 cm unlikely (see, *e.g;* Magnan 2024). Since those grains are at the boundary between the two drag regimes, we can reasonably use the Epstein drag law for every grain.

5.2.2. *End of the collapse*

We shall see in §6 that the gas density increases by several orders of magnitude during the collapse. The gas' mean free path eventually becomes smaller than even the smallest grains, allowing us to use the Stokes drag law for every grain.

[1] The factor 9/4 at the front ensures a smooth transition between the two drag regimes

5.3. *Stopping times*

5.4. *What do the sound waves look like?*

We claimed in §3 that the sound speed is reduced by a factor $\sqrt{\mu+1}$ within the clump. This statement is only valid in well-coupled gas/dust mixtures, and in dust-dominated mixtures such as our clump, the condition for strong coupling is that the gas stopping time be shorter than the period of (standard) sound waves. Of course, short-wavelength waves are high-frequency, so they cannot be well coupled. But the sound waves that are most likely to affect collapse are the clump-scale waves of wavenumber $k \sim 1/R$.

5.5. *Caveats*

The transition phase between Epstein, Stokes and turbulent drag remains to be studied. However, if the transition is very short, only the Epstein and turbulent regimes may need to be considered.

6. GAS DYNAMICS

6.1. *Is the gas static?*

Even though dust slows down the sound waves, the sound crossing time remains shorter than the free-fall time. In those conditions, Jeans' criterion suggests that the gas should not collapse. Segretain et al. (2024) seem to confirm this, as well as Shariff & Cuzzi (2015). Indeed, they introduce $J = (32/3\pi)\,(t_\mathrm{s}/t_\mathrm{ff})^2$ and find static gas when $J < 0.025$, compressive bounces when $0.1 < J < 0.3$, and free-fall collapse when $J_t > 0.4$. We expect most clumps to start in the first regime.

The goal of the present subsection is to acknowledge the intricacies of this static-gas phase, before providing a tentative model for this phase's dynamics.

Since the gas stopping time is much smaller than the free-fall time, we expect that when the dust velocity changes, the gas adapts its velocity and establishes a new terminal velocity difference in just a few gas stopping times. But since the sound crossing time is much smaller than the free-fall time, we also expect a process of hydrostatic adjustment (Horace 1909; Guiraud & Zeytounian 1982; Bannon 1995). Essentially, when the dust moves towards the center of the clump, it acts as a piston on the gas and it steepens the potential well. By modifying both the pressure gradient and the gravitational field, it nudges the gas out of hydrostatic balance. The gas responds to this perturbation by emitting sound waves. Those redistribute gas masses, thereby re-establishing a new hydrostatic equilibrium. Unfortunately, those two processes seem to be in conflict: the first one would fix the gas velocity to a terminal value on the gas stopping timescale, whereas the second one

would requires gas velocities perturbations to survive for several sound crossing times.

One way to resolve this paradox is to invoke small-wavelength sound waves. Indeed, they have a short enough period to decouple from the dust. Yet, we do not think short waves are the correct solution. Indeed, Jeans' analysis suggests that they would not be able to support the clump against gravitational collapse. In other words, we think that hydrostatic adjustment is mediated by clump-scale waves.

At those scales, the gas is well-coupled to the dust. We show in §B that it is still able emit sound waves, but that those sound waves are slower than usual and damped over time.

The first point of concern is wave damping. Indeed, if it occurs on the gas stopping time, then no wave remains to establish hydrostatic balance on the sound crossing time. Fortunately, if the dust is well coupled to a sound wave, this wave introduces very little perturbation in relative velocity. This allows the clump-scale waves to bypass the terminal velocity constraint and to survive for several sound crossing times.

The flip side of the coin is that since terminal velocities are small, the sound waves must displace not just the gas, but also the dust. This means that hydrostatic adjustment affects the gas and dust densities alike. This specific issue warrants further work, and will be pursued in a separate future paper.

7. TURBULENCE

7.1. *Kolmogorov and α scalings*

In α-model of Shakura & Sunyaev (1973), turbulence is forced at the disc scale according to

$$l_f = \sqrt{\alpha}\, H, \quad t_f = \Omega^{-1}, \quad v_f = \sqrt{\alpha}\, c_\mathrm{s},$$

This triggers an energy cascade towards small scales. If disc turbulence was homogeneous and isotropic, its inertial range would follow (Kolmogorov 1941a,b,c,d)

$$t_i \propto l_i^{2/3}, \quad v_i \propto l_i^{1/3},$$

The cascade stops once the eddies are small and slow enough to be dissipated by molecular viscosity. Setting the Reynolds number to one at the dissipation scales gives

$$l_d = \left(\frac{c_\mathrm{s}\,\lambda^3}{\alpha\,\Omega}\right)^{1/4}, \quad t_d = \left(\frac{\lambda}{\alpha\, c_s\,\Omega}\right)^{1/2}, \quad v_d = \left(c_\mathrm{s}^3 \lambda \alpha \Omega\right)^{1/4}.$$

These are all the scales of turbulence we will consider in our system. Eddies of clump scale fall into the inertial range.

7.2. *Should we include a turbulent viscosity term?*

Here we will consider three different scales of eddies and argue that none of these are able to penetrate the clump and create any eddies within the clump. First, turbulent eddies on the forcing scale will effectively act as a wind on the entire clump (see Section 2.2.1) and for most starting radii, this will not significantly strip any material from the clump. The next eddies to consider are in the inertial range, on the order of the clump size. The gas in this instance will be well-coupled to the dust clump, and as a result will have a very short stopping time

$$t_g = \frac{\rho_d}{\rho_g} t_s\,, \tag{33}$$

since the dust-to-gas ratio is much larger than 1. As a result of this short stopping time, the gas will only be able to penetrate the top layer of the dust clump before coming to a stop. As a result, smaller eddies will only form in these layers of the dust clump and not the majority of it. Finally, smaller eddies on the order of the dissipation scale may be less well coupled to the dust, however these are much smaller and slower, so will not have time to fully penetrate into the clump before it has finished collapsing. Furthermore, as the collapse progresses, the dust-to-gas ratio will only increase, further decreasing the gas stopping time and reducing the ability for any eddies to enter the clump.

7.3. *Should we include a dust diffusion term?*

Since we do not expect that any significant gas turbulence will be present in the majority of the clump, dust diffusion within the clump can be neglected.

7.4. *Caveats*

In this section we do not consider any other sources of turbulence. The collapse process itself could drive turbulence in the clump, which might then have a considerable effect on the dust during the collapse. This will be considered in future work.

8. CONCLUSION

ACKNOWLEDGMENTS

This work originated from a project of the Summer Program in Astrophysics 2025 held at the University of Virginia, and funded by the Center for Global Inquiry and Innovation, the National Science Foundation (Grant 2452494), the National Radio Astronomy Observatory (NRAO), the Kavli Foundation and the Heising-Simons Foundation. We also wish to thank all the participants for eye-opening discussions.

DATA AVAILABILITY

No new data were generated or analysed in support of this research. We intend to publicly release the code on GitHub when we publish the paper.

APPENDIX

A. PARAMETERS

We computed many orders of magnitude in the core of the paper, but to make things readable we did not always provide the values we used for the parameters. The goal of the present appendix is to remediate this.

A.1. *The gas*

We work with pure dihydrogen of adiabatic index $\gamma = 1.4$, mean molecular weight $m_\mathrm{g} \approx 3.34 \times 10^{-27}\,\mathrm{kg}$, kinetic diameter $d = 2.9 \times 10^{-10}\,\mathrm{m}$, and specific heat capacity $c_{\mathrm{p,g}} \approx 1.4 \times 10^4 \mathrm{J/kg/K}$.

A.2. *Disc model*

We use the model of Chiang & Youdin (2010),

$$T = \overline{T} \left(\frac{r}{1\,\mathrm{AU}}\right)^{-q},$$
$$\Sigma_\mathrm{g} = \overline{\Sigma}_\mathrm{g} \left(\frac{r}{1\,\mathrm{AU}}\right)^{-p},$$

where $\overline{T} = 120\,\mathrm{K}$ and $\overline{\Sigma}_\mathrm{g} = 2.2 \times 10^4\,\mathrm{kg/m^2}$ are the temperature and surface density scales, $q = 3/7$ and $p - 3/2$ are the power law indices, and r is the distance between the star and the clump. Note that $\gamma = 1 + q/p$, as expected.

From there, we can use the kinetic theory of gases to deduce the sound speed

$$c_\mathrm{s} = \sqrt{\frac{\gamma\, k_\mathrm{B} T}{m_g}} = 8 \times 10^2 \left(\frac{r}{1\,\mathrm{AU}}\right)^{-q/2} \mathrm{m/s},$$

the gas mean free path

$$\lambda = \frac{1}{\sqrt{2}\pi\, n_\mathrm{g}\, d^2} = 1.6 \times 10^{-3} \left(\frac{r}{1\,\mathrm{AU}}\right)^{p+3/2-q/2} \mathrm{m},$$

and the kinematic viscosity

$$\nu = c_\mathrm{s}\, \lambda = 1.3 \times 10^{-2} \left(\frac{r}{1AU}\right)^{p+3/2-q} \mathrm{m^2/s}.$$

We work with a solar-mass star, so $M_* = 2 \times 10^{30}\,\mathrm{kg}$. From there, we deduce the orbital frequency

$$\Omega = \frac{GM_*}{r^3} = 2.0 \times 10^{-7} \left(\frac{r}{1\,\mathrm{AU}}\right)^{-3/2} \mathrm{s^{-1}}, \tag{A1}$$

the gas scale height

$$H_\mathrm{g} = c_\mathrm{s}/\Omega = 4 \times 10^9 \left(\frac{r}{1\mathrm{AU}}\right)^{-q/2+3/2} \mathrm{m},$$

the gas density

$$\rho_\mathrm{g} = \frac{\Sigma_\mathrm{g}}{\sqrt{2\pi} H_\mathrm{g}} = 2.2 \times 10^{-6} \left(\frac{r}{1\mathrm{AU}}\right)^{-p+q/2-3/2} \mathrm{kg/m^3},$$

and the gas number density

$$n_{\rm g} = \rho_{\rm g}/m_{\rm g} = 6.6\times10^{20}\left(\frac{r}{1{\rm AU}}\right)^{-p+q/2-3/2}\ {\rm particles/m^3},$$

To avoid confusion, let us stress that those orders of magnitude are only valid at the start of the collapse. As the gas compresses, $\rho_{\rm g}$ and $n_{\rm g}$ increase while λ and ν decrease.

Finally, we assume that the α parameter governing the strength of the turbulence is of order 10^{-4}.

A.3. *The dust*

We work with pure silicate grains of density $\rho_{\rm s} = 1.0\times10^3\,{\rm kg/m^3}$, thermal diffusivity $\kappa_{\rm s} = 1.4\times10^{-6}\,{\rm m^2/s}$, and specific heat capacity $c_{\rm p,s} = 1.2\times10^3\,{\rm J/K/kg}$.

As discussed in §5.2, there is some debate as to the size of the grains at the start of the collapse, so we prefer to keep the grain radius a unconstrained.

A.4. *The initial clump*

Simulations of the streaming instability produce clumps with a distribution of masses (Simon et al. 2016; Schäfer et al. 2017; Abod et al. 2019; Klahr & Schreiber 2020). This is probably true of all other clump formation mechanisms, hence why we prefer to leave the clump mass unconstrained. That being said, we find that due to the astronomical numbers involved, it is easier to have an intuition about planetesimal radii than planetesimal masses, so our free parameter is really $R_{\rm p}$ rather than $M = \frac{4}{3}\pi\rho_{\rm s}R_{\rm p}^3$.

As discussed in §2, we start the collapse once erosion via the tidal shear, turbulent eddies, and the azimuthal headwind become negligible. In practice, this means that initial radius R_0 is a fraction X_0 of the Hill radius.

$$R_{\rm H} = r\left(\frac{M}{3M_*}\right)^{1/3} = 1.3\times10^2\left(\frac{r}{1{\rm AU}}\right)R_{\rm p}\,{\rm m}.$$

From there, we can deduce the initial dust density

$$\rho_{\rm d} = \frac{M}{\frac{4}{3}\pi R_0^3} = 4.2\times10^{-4}\left(\frac{r}{1{\rm AU}}\right)^{-3}X_0^{-3}\,{\rm kg/m^3},$$

the initial dust-to-gas ratio

$$\mu = \frac{\rho_{\rm d}}{\rho_{\rm g}} = 1.9\times10^2\left(\frac{r}{1{\rm AU}}\right)^{p-q/2-3/2}X_0^{-3},$$

and the initial dust number density

$$n_{\rm d} = \frac{\rho_{\rm d}}{\frac{4}{3}\pi\rho_{\rm s}a^3} = 1.0\times10^{11}\left(\frac{r}{1{\rm AU}}\right)^{-3}X_0^{-3}\left(\frac{a}{1\mu{\rm m}}\right)^{-3}\ {\rm particles/m^3}.$$

B. GRAVITATIONAL INSTABILITY AND SOUND WAVES IN A DUST-LADEN FLUID

We have studied the Jean's instability of uniform medium with dust and gas for arbitrary particle stopping times, t_s, and dust to gas density ratios $\epsilon = \rho_p/\rho_g$. The strength of self-gravity is length scale dependent. We use

$$\lambda_{\rm J,g}^2 = \frac{4\pi G\rho_g}{(c_s k)^2} \tag{B2}$$

as the usual ratio of wavelength to Jean's wavelength squared, with c_s the gas sound-speed and k the wavenumber of the perturbation.

We use the frequency of a pure gas sound wave $\tilde{\omega}_g = c_s k$, to define a scaled frequency $\omega = \tilde{\omega}/\tilde{\omega}_g$. For a self-gravitating pure gas the dispersion relation $\omega^2 = 1 - \lambda^2_{\rm J,g}$ gives the usual gas Jean's criterion for instability as $\lambda_{\rm J,g} > 1$.

The particle stopping time, t_s, can be dimensionally scaled as $\tau = t_s \tilde{\omega}_g$, or more relevantly scaled to the particle free-fall time $t_{ff,p} = 1/\sqrt{4\pi G \rho_p}$ as $t_s/t_{\rm ff,p} = \tau \lambda_{J,g} \sqrt{\epsilon}$.

We summarize our main findings. The relevant Jeans parameter for a well coupled gas dust mixture is $\lambda_{J,m} = \lambda_{J,g}(1+\epsilon)$, which includes the augmentation of self-gravity and the reduction of the sound speed by coupled solids. As $\tau \to 0$, the dispersion relation approaches

$$\omega^2 = \frac{1}{1+\epsilon} - (1+\epsilon)\lambda^2_{J,g} \tag{B3}$$

i.e. instability of the coupled mixture for $\lambda_{J,m} > 1$. The collapse rate for $\lambda_{J,m} \gg 1$ is

$$\sigma t_{\rm ff,p} = \sqrt{\frac{1+\epsilon}{\epsilon}} \tag{B4}$$

For finite, $t_s \ll t_{ff,p}$ there is also a settling mode which grows at a rate

$$\sigma t_{ff,p} \simeq \frac{1}{1-\lambda^2_{J_m}} \frac{t_s}{t_{ff,p}} \tag{B5}$$

This rate is only valid for $\lambda_{J,m} < 1$ by a safe margin. Across $\lambda_{J,m} \sim 1$, the gravitational collpase rate smoothly connects Eq. B5 to Eq. B4.

For the loose coupling regime of $t_s \gg t_{ff,p}$, growth is always on a free fall timescale with

$$\sigma t_{\rm ff,p} \simeq 1 \tag{B6}$$

for $\lambda_{\rm J,m} < 1$. For $\lambda_{\rm J,m} \gg 1$, the coupled collapse rate of Eq. B4 again applies. When $\epsilon \gg 1$ the transition from particle-only free fall to joint particle and gas free-fall is negligible in terms of rate.

In summary there are three relevant collapse rates, σ. Eq. B4 for $\lambda_{J,m} > 1$ (independent of t_s). And for $\lambda_{J,m} < 1$, Eq. B5 holds for $t_s \ll t_{ff,p}$ and Eq. B6 for $t_s \gg t_{ff,p}$. All rates connect smoothly across $t_s = t_{ff,p}$ and $\lambda_{J,m} = 1$.

While the behavior of unstable modes is simple to describe, and most relevant, the behavior of sound waves is quite rich for $\epsilon \ll 1$, with or without self-gravity. In short strong drag on the gas with $\epsilon \sim \tau$ damps sound waves, with no propagating modes. Also for loose coupling, particle selfgravity promotes the propagation of sound waves. Physically, in these modes the particle density is out of phase with the gas density. Thus while gas self-gravity decelerates sound waves (lowering the frequency of sound waves as in the usual Jeans dispersion relation), particle self gravity in these modes accelerates the sound waves in these modes. It's unclear if this rich behavior of sound waves is ever relevant as the collapsing modes should be the most relevant.

REFERENCES

Abod, C. P., Simon, J. B., Li, R., et al. 2019, ApJ, 883, 192, doi: 10.3847/1538-4357/ab40a3

Bannon, P. R. 1995, Journal of the Atmospheric Sciences, 52, 1743, doi: 10.1175/1520-0469(1995)052<1743:HALP>2.0.CO;2

Birnstiel, T., Ormel, C. W., & Dullemond, C. P. 2011, Astronomy and Astrophysics, 525, A11, doi: 10.1051/0004-6361/201015228

Chiang, E., & Youdin, A. N. 2010, Annual Review of Earth and Planetary Sciences, 38, 493, doi: 10.1146/annurev-earth-040809-152513

Cuzzi, J. N., Hogan, R. C., & Bottke, W. F. 2010, Icarus, 208, 518, doi: 10.1016/j.icarus.2010.03.005

Guiraud, J. P., & Zeytounian, R. K. 1982, Tellus, 34, 50, doi: 10.1111/j.2153-3490.1982.tb01791.x10.3402/tellusa.v34i1.10786

Haberle, R. M., Kahre, M. A., Bertrand, T., & Wolff, M. J. 2025, Icarus, 429, 116452, doi: 10.1016/j.icarus.2024.116452

Hopkins, P. F., & Squire, J. 2018, MNRAS, 480, 2813, doi: 10.1093/mnras/sty1982

Horace, L. 1909, Proceedings of the London Mathematical Society, s2-7, 122, doi: https://doi.org/10.1112/plms/s2-7.1.122

Klahr, H., & Schreiber, A. 2020, ApJ, 901, 54, doi: 10.3847/1538-4357/abac58

Kobayashi, H., & Tanaka, H. 2021, The Astrophysical Journal, 922, 16, doi: 10.3847/1538-4357/ac289c

Kolmogorov, A. 1941a, Akademiia Nauk SSSR Doklady, 30, 9

—. 1941b, Akademiia Nauk SSSR Doklady, 31, 319

—. 1941c, Akademiia Nauk SSSR Doklady, 32, 16

—. 1941d, Akademiia Nauk SSSR Doklady, 33, 299

Lissauer, J. J., & Stewart, G. R. 1993, in Protostars and Planets III, ed. E. H. Levy & J. I. Lunine, 1061

Magnan, N. 2024, PhD thesis, University of Cambridge, doi: 10.17863/CAM.117047

Morbidelli, A., & Nesvorny, D. 2020, 25–59, doi: 10.1016/B978-0-12-816490-7.00002-3

Ormel, C. W., & Klahr, H. H. 2010, A&A, 520, A43, doi: 10.1051/0004-6361/201014903

Schäfer, U., Yang, C.-C., & Johansen, A. 2017, A&A, 597, A69, doi: 10.1051/0004-6361/201629561

Segretain, P., Méheut, H., Moreira, M., et al. 2024, A&A, 692, A118, doi: 10.1051/0004-6361/202451447

Shakura, N. I., & Sunyaev, R. A. 1973, A&A, 24, 337

Shariff, K., & Cuzzi, J. N. 2015, ApJ, 805, 42

Simon, J. B., Armitage, P. J., Li, R., & Youdin, A. N. 2016, ApJ, 822, 55, doi: 10.3847/0004-637X/822/1/55

Weidenschilling, S. J. 1977, MNRAS, 180, 57, doi: 10.1093/mnras/180.2.57

Youdin, A., & Johansen, A. 2007, ApJ, 662, 613, doi: 10.1086/516729

Youdin, A. N., & Goodman, J. 2005, ApJ, 620, 459, doi: 10.1086/426895